The effects of interannual climate variability on the moraine record

Leif S. Anderson[1], Gerard H. Roe[2], and Robert S. Anderson[1]

[1] Institute of Arctic and Alpine Research and Department of Geological Sciences, University of Colorado, Campus Box 450, Boulder, Colorado 80309, USA

[2]Department of Earth and Space Sciences, University of Washington, 4000 15th Ave. NE, Seattle, Washington 98195, USA

ABSTRACT

Glacial moraines are commonly used to infer mean climate conditions (annual precipitation and melt-season temperature) at the time of moraine formation. However, recent research has demonstrated that substantial fluctuations in glacier length also occur in response to stochastic, year-to-year variability in mass balance. When interpreting moraine sequences it is important to differentiate between moraines that reflect the signal of actual climate changes versus those that may reflect the noise of interannual climate variability. We address this issue for the glaciers of the Colorado Front Range, USA. Using a linear glacier model that allows for a thorough exploration of parameter uncertainties, supplemented by a shallow-ice flowline model, our analyses suggest that i) nested LGM moraine sequences are often confined to a range of glacier lengths that can be attributed to interannual climate variability; ii) mean glacier lengths are ~10-15% up valley from maximum glacier lengths; and iii) glaciers smaller than 6 km^2 were likely transient features, coming and going due to interannual variability.

INTRODUCTION

Glacial to interglacial changes in the long-term averages of annual precipitation (P) and melt-season temperature (T) are sufficient, in many places, to drive large changes in glacier length, as recorded by the emplacement of terminal moraines. But the natural, year-to-year (interannual), fluctuations of P and T have also been shown to force kilometer-scale glacial length fluctuations, due solely to the random alignment of years of negative and positive mass balance, even in steady climates (e.g., Oerlemans, 2001; Reichert et al., 2002; Roe and O'Neal, 2009). A steady climate implies constant long-term averages ($\equiv \overline{P}, \overline{T}$) and, importantly, constant standard deviations ($\equiv \sigma_P, \sigma_T$). Interannual variability is due to the stochastic fluctuations of weather and internal modes of variability such as the North Atlantic, the Pacific/North American, and the El Niño-Southern Oscillations. The amplitude of interannual variability varies with location and climate state, but it is always present. If we are to accurately constrain the values of past $\overline{T}$ and $\overline{P}$ using glacier moraines we must understand the effects of this unavoidable year-to-year climate variability on glacier length and moraine emplacement.

To illustrate the problem, consider two glaciers: (a) a glacier subject to constant $\overline{T}$ and $\overline{P}$ forms a steady ice-surface profile that terminates at a steady, mean length, $\overline{L}$ (Fig. 1A); and (b) a glacier subject to a climate with the same $\overline{T}$ and $\overline{P}$ but that also includes interannual variability. The glacier of case (b) will produce a terminus history that will fluctuate around the same $\overline{L}$ as glacier (a) (Fig. 1B; Fig. 2B). However, for glacier (b) $\overline{L}$ is a theoretical length with no expression in the landscape, and is the location around which the terminus fluctuates. If we assume that i) glacial length maxima represent potential moraine-forming locations, ii) terminal moraines can be formed on 10-20 year timescales (see DR.3), iii) terminal moraines do not limit the extent of subsequent advances, and iv) all moraines that are overrun by subsequent advances are removed, then the maximum excursion from $\bar{L}$, will form the furthest terminal moraines (see DR.3 for a detailed discussion). Estimates of average climate (i.e., $\bar{P}, \bar{T}$) should be based on $\bar{L}$ rather than L_{max} (Fig. 1B). Thus, we face the challenge of estimating $\bar{L}$ knowing only the glacier geometry preserved by the L_{max} advance, while also accounting for the substantial uncertainties in the mass balance, geometry, and glacier parameters that pertained in past climates.

We focus on the last glacial maximum (LGM) moraine record in the Colorado Front Range, USA, because of well-dated, nested sets of near-LGM moraines, diverse glacier geometries, and the availability of long-term, high-elevation modern meteorological records. We first employ a dynamic flowline model to confirm, in accordance with prior work in other settings, that interannual variability can drive significant length fluctuations. The focus however is on using a linearized model to more efficiently explore a wide range of parameter uncertainty.

MODEL DESCRIPTIONS

Flowline Model

We follow standard equations for the shallow-ice-approximation incorporating glacier sliding (e.g., Oerlemans, 2001):

$$\frac{dH(x)}{dt} = \dot{b}(x) - \frac{dF(x)}{dx};\; F(x) = \rho^3 g^3 \left(f_d H(x)^2 + f_s\right) H(x)^3 \left(\frac{dz_s}{dx}\right)^3, \qquad (1)$$

where $H(x)$ is ice thickness at position x, $\dot{b}(x)$ is the local net mass balance, $F(x)$ is the depth-integrated ice flux, ρ is ice density, g is the acceleration due to gravity, dz_s/dx is the local ice surface slope, $f_d = 1.9 \times 10^{-24}$ Pa^3 s^{-1} and $f_s = 5.7 \times 10^{-20}$ Pa^3 m^2 s^{-1}.

Linearized Model

The linear model used in this study considers the conservation of mass, neglects ice dynamics, and, in a steady climate, considers length variations as departures from a mean length $\bar{L}$ that are small enough that the system is linear (Roe and O'Neal, 2009). Using finite differences to discretize the governing equation and using a time step Δt of 1 year, the response of the glacier to stochastic climate variability is

$$L'_{t+\Delta t} = L'_t\left(1 - \frac{\Delta t}{\tau}\right) + \beta\sigma_P\nu_t + \alpha\sigma_T\lambda_t \quad , \qquad (2)$$

where subscript t denotes the year; ν_t and λ_t are independent normally distributed random processes; and α and β are coefficients that are functions of glacier geometry:

$$\alpha = -\frac{\mu A_{T>0}\Delta t}{wH}, \ \beta = \frac{A_{tot\Delta t}}{wH}, \qquad (3,4)$$

where,

$$A_{T>0} = A_{abl} + \frac{Pw}{\mu\Gamma\tan\phi} \ . \qquad (5)$$

Parameter definitions are given in Table 1. The characteristic timescale τ for the linear model is

$$\tau = \frac{wH}{\mu\Gamma\tan\phi A_{abl}} \ , \qquad (6)$$

the time over which the glacier 'remembers' past T and P states. Derivation of these governing equations is given in the appendix of Roe and O'Neal (2009).

Climate Data and Parameter Selection

Meteorological data were extracted from the longest-running high-elevation weather station in North America on Niwot Ridge, CO (see Figure 3B; Station D1; 1952-2010; 3743m a.s.l). Assuming that the melt season runs from June to September, we determined that ($\bar{T}$, σ_T) is (6.3,1.3) °C and for annual precipitation ($\bar{P}$, σ_P) is (1.2, 0.22) m a^{-1}. Data were linearly detrended. While the modern summertime near-surface lapse rate in the ice-free Boulder Creek catchment is -5.6 °C km^{-1} (Pepin and Losleben, 2002), we consider a range based on a global compilation of summer on-ice, near-surface lapse rates which for valley glaciers has a mean of 4.0±2.1°C km^{-1} (1σ) (Table 1; DR.1). We constrain the melt-factor, μ (i.e., ablation per 1°C change in T), based on a global compilation of μ for snow (4.5±1.7 mm °Cday^{-1}) and ice (7.7±3.2 mm °Cday^{-1}) (see DR.2). We also consider a relatively broad range of accumulation-area ratios (AAR), the ratio of the accumulation area to the total glacier area, from 0.5 to 0.8 (Meier and Post, 1962).

We define climate as the statistics of weather, averaged over any interval relevant for the question at hand (typically longer than 30 years). The duration of the regional LGM climate is defined by the parameter D, for which we consider a broad range between 500 and 7500 years, the upper limit being the duration of the LGM sea level low stand (26.5 to 19 ka; Clark et al., 2009). Alternatively, a natural choice for D is the time interval separating two dated moraines we wish to attribute to either climate change or climate variability.

IMPACT OF INTERANNUAL VARIABILITY ON MEAN GLACIER LENGTH

The flowline model (eq. 1) was integrated with mid-range parameters (Table 1) for the basal slope and length of Fall Creek glacier (Table 2). The most likely parameter set generated a standard deviation of length fluctuations (σ_L) of 370 m. Sample model output is shown in Fig. 2C. For the linear model eqs. 3&4 can be solved exactly for σ_L

$$\sigma_L = \sqrt{\frac{\tau \Delta t}{2}} \sqrt{\alpha^2 \sigma_T^2 + \beta^2 \sigma_P^2}\,. \qquad (7)$$

For the same parameters as the flowline model, the linear model gives σ_L= 415m, consistent with the ~15% overestimate described and explained by Roe (2011). This inter-model difference is much smaller than the uncertainty range of the parameters (Table 1). The outer bounds of σ_L for the linear model are 180 and 800 m, representing cases in which all parameters are simultaneously given their extreme values. Beyond its simplicity, a clear value of the linear model, as seen in eq.7, is that parameter uncertainty can be straight-forwardly propagated: a high sensitivity to T or P (i.e., large α or β), or a long response time leads to a large σ_L.

Roe (2011) derived excursion statistics for glaciers driven by climate variability (following standard texts, e.g., Vanmarcke, 1983; see also Reichert et al. 2002), which we adapt here. In any given time interval D the maximum excursion, L_{max} cannot be known exactly, but it is described by a probability distribution. Roe (2011) showed that the most likely L_{max} can be related to the average position, $\bar{L}$, by

$$\bar{L} = L_{\max} - \sigma_L \sqrt{2 \ln\left(\frac{D\dot{\sigma}_L}{2\pi\sigma_L \ln(2)}\right)}\ , \qquad (8)$$

where $\dot{\sigma}_L$ is the standard deviation of the time rate of change of glacier length (see eq. 9 and A8 in Roe (2011) with p = 0.5). Equation 8 is quite general, and holds provided the probability distribution of glacier fluctuations is normally distributed (Fig. 1B), and has been shown to govern the variability of terminus position in flowline glacier models (see Reichert et al., 2002; Roe, 2011). Roe (2011) further demonstrated that setting $\sigma_{\dot{L}} = \sigma_L \sqrt{2/\psi\tau\Delta t}$ emulated the behavior of a standard numerical flowline model, where ψ (≈10) is a factor introduced because high frequencies are damped more strongly in a numerical flowline model than is predicted by the linear model. Because ψ is passed through two square roots and a natural log in eq. 8, the effect of varying this parameter is minimal. A doubling or halving of ψ results in a $\pm$ 0.6% change in $\overline{L}$ when D is larger than the glacier response time, τ.

Mean Length and Signal-to-Noise Results

Table 2 shows the linear model mean-length results for eleven LGM glaciers from the Colorado Front Range. For glaciers with area greater than 6 km^2, the most likely mean glacier length is 10-15% back from L_{max}. Bounds on the potential location of the mean length—3% to 50% — represent cases in which all parameters are simultaneously given their extreme values. As this is unlikely, the resulting range should be considered very much an outer bound on the mean length.

Interpreting the cause of glacier length changes requires that we discern the competing influences of a signal (a change in $\overline{P}$ or $\overline{T}$ leading to a change in $\overline{L}$) (Fig. 1B; eq. 8) and a noise component (climate noise σ_P, σ_T driving length fluctuations, σ_L) (Fig. 1B; eq. 7). Comparison of the $\overline{L}$ and the σ_L components for modeled LGM glaciers with area greater than 6 km^2 shows that it is likely that larger glaciers persisted throughout the local LGM, as their $\overline{L}$ was much larger than their σ_L (Table 2). Glaciers with area less than 6 km^2 likely flickered in and out of existence due to the interannual variability of the (colder) LGM climate, as $\overline{L}$ was of comparable size to σ_L .

DISCUSSION

Moraines reflect maximum advances, and our results suggest that climate noise can drive such advances substantially beyond what the mean climate conditions would support (Fig 1B; Fig. 2D). Climate estimates derived from maximum glacier geometries do not represent the local LGM-mean climate. Rather, they have a one-sided bias due to stochastic excursions away from the mean. Equilibrium-line-altitudes (ELAs) and climate change estimates from glacier models directly reconstructed from maximum moraines will therefore overestimate the climate change. In our setting, the central parameter range suggests this is a 10-15% effect for LGM moraines. Because moraines reflect maximum advances, dating the maximum terminal moraine provides a minimum estimate of when a climate change initiated. Furthermore, constraining the timing of retreat from the estimated mean length provides an estimate of when a climate change terminated (e.g., Young et al., 2011).

The role of interannual variability in driving stochastic glacier length fluctuations is important to consider for two additional reasons: the formation of LGM nested moraine sequences in individual valleys; and the asynchronous timing of LGM advances across the western US. Broad LGM terminal moraine complexes (sets of closely spaced or nested terminal moraines in a single valley; Fig. 1B; Fig. 2C; Fig. 3C; DR.4) possibly represent cycles of kilometer-scale retreat and re-advance that are independent of true climate change. It follows that such a glacier likely formed one moraine, then left the terminal moraine complex and returned, forming a second moraine. Terminal moraines between $\overline{L}$ and L_{max} are therefore not likely 'recessional' moraines in the classic sense. If we expect 10-15% advances from the mean glacial length, we should also expect 10-15% retreats (Fig. 1B; Fig. 2C) that are unlikely to form moraines. The potential for exposure of bedrock between L_{max} and L_{min} during these cycles could impact the interpretation of cosmogenic radionuclide-derived bedrock exposure ages.

It is also possible that the natural variation of glacial length about its mean could explain the spread of ages derived from LGM maximum terminal moraines across the Western US (Fig. 2D; see Young et al., 2011; Thackray, 2008; Licciardi et al., 2004 for other interpretations), and even globally (Schäfer et al., 2006). Incoherent patterns of interannual variability from region-to-region could have resulted in glacier advances and retreats at different times around the Western US during the regional LGM. Modern snowpack snow-water-equivalent anomalies support the above hypothesis, as they are coherent over a several hundred-kilometer length scale that is significantly smaller than the glaciated area within the Western US (Cayan, 1996; Huybers and Roe, 2009).

By exploring a very wide parameter space, we have constrained the effects of interannual variability on glacial length and moraine formation over extreme bounds. The range of parameter uncertainty could be better constrained by examining how the climate parameters vary in space from the LGM to the present. The most uncertain climate parameters, Γ, σ_P, and σ_T, could be better constrained by using atmospheric circulation model output, and better minimum estimates of D could be obtained by reducing the uncertainty in moraine-derived dates. It should also be determined if using higher order ice physics models changes the effects of interannual variability on glacier length, although we anticipate that parameter uncertainty will swamp any differences between models. In the climate forcing presented here, we have assumed that T and P are uncorrelated from year-to-year (white noise), as is generally the case for centennial-scale instrumental observations of T and P and glacier mass balance records (e.g., Burke and Roe, 2013); on longer time-scales, paleoclimate records show that a degree of persistence (correlation from year-to-year) does exist (e.g., Huybers and Curry, 2006). Even a small degree of persistence can substantially increase the magnitude of fluctuations (e.g. Reichert et al., 2001). For this reason and others outlined in Roe and O'Neal (2009), we feel that our estimates of the fluctuation of glacier length about the mean length are conservative.

CONCLUSIONS

We have assessed the effects of interannual variability on glacier length and its associated uncertainty in a continental climate during the LGM. Interannual variability inevitably results in glacial length fluctuations around a mean glacier length. The maximum excursion from the mean length is responsible for the formation of LGM terminal moraines that are, in the Colorado Rockies, most likely 10-15% down valley from the mean LGM glacier length, with maximum bounds of 50%-3%. Glacier length fluctuations forced by interannual variability can be viewed as a smaller scale example of the moraine survival problem, e.g. Gibbon et al. (1984), with consequences for the interpretation of moraine complexes. Both standard flowline and linear model results support the fundamental conclusions of this study. Glacier length fluctuations due to year-to-year climate variability should therefore be included in the interpretation of the moraine record in order to realize the record's full potential.

ACKNOWLEDGMENTS

We thank the Niwot Ridge Long Term Ecological Research for weather station data. L.S.A. acknowledges support from NSF DGE-1144083 (GRFP). R.S.A. acknowledges support of NSF EAR-1239281 (Boulder Creek CZO).

REFERENCES CITED

Burke, E.E., and Roe, G.H., 2013, The absence of memory in the climatic forcing of glaciers: Climate Dynamics, p. 1-12, doi: 10.1007/s00382-013-1758-0.

Cayan, D.R., 1996, Interannual Climate Variability and Snowpack in the Western United States: Journal of Climate, v. 9, p. 928–948.

Clark, P.U., Dyke, A.S., Shakun, J.D., Carlson, A.E., Clark, J., Wohlfarth, B., Mitrovica, J.X., Hostetler, S.W., and McCabe, A.M., 2009, The Last Glacial Maximum: Science (New York, N.Y.), v. 325, no. 5941, p. 710–4, doi: 10.1126/science.1172873.

Gibbons, A.B., Megeath, J.D., and Pierce, K.L., 1984, Probability of moraine survival in a succession of glacial advances: Geology, v. 12, p. 327–330.

Huybers, P., and Curry, W., 2006, Links between annual, Milankovitch and continuum temperature variability: Nature, v. 441, no. 7091, p. 329–32, doi: 10.1038/nature04745.

Huybers, K., and Roe, G.H., 2009, Spatial Patterns of Glaciers in Response to Spatial Patterns in Regional Climate: Journal of Climate, v. 22, no. 17, p. 4606–4620, doi: 10.1175/2009JCLI2857.1.

Licciardi, J.M., Clark, P.U., Brook, E.J., Elmore, D., and Sharma, P., 2004, Variable responses of western U.S. glaciers during the last deglaciation: Geology, v. 32, no. 1, p. 81, doi: 10.1130/G19868.1.

Meier, M.F., and Post, A.S., 1962, Recent Variations in mass net budgets of glaciers in western North America, *in* IASH Publication, p. 63–77.

Oerlemans, J., 2001, Glaciers and Climate Change: Taylor and Francis, 160 p.

Pepin, N., and Losleben, M., 2002, Climate change in the Colorado Rocky Mountains: free air versus surface temperature trends: International Journal of Climatology, v. 22, no. 3, p. 311–329, doi: 10.1002/joc.740.

Porter, S.C., Pierce, K.L., and Hamilton, T.D., 1983, Late Wisconsin mountain glaciation in the western United States, *in* Porter, S.C., ed., Late Quaternary environments in the western United States. The late Pleistocene, volume 1: Minneapolis, University of Minnesota Press, p. 71–111.

Reichert, B.K., Bengtsson, L., and Oerlemans, J., 2002, Recent glacier retreat exceeds internal variability: Journal of Climate, v. 15, no. 21, p. 3069–3081, doi: 10.1175/1520-0442(2002)015<3069:RGREIV>2.0.CO;2.

Roe, G.H., 2011, What do glaciers tell us about climate variability and climate change?: Journal of Glaciology, v. 57, no. 203, p. 567–578, doi: 10.3189/002214311796905640.

Roe, G.H., and O'Neal, M.A., 2009, The response of glaciers to intrinsic climate variability: observations and models of late-Holocene variations in the Pacific Northwest: Journal of Glaciology, v. 55, no. 193, p. 839–854, doi: 10.3189/002214309790152438.

Schäfer, J.M., Denton, G.H., Barrell, D.J. a, Ivy-Ochs, S., Kubik, P.W., Andersen, B.G., Phillips, F.M., Lowell, T. V, and Schlüchter, C., 2006, Near-synchronous interhemispheric termination of the last glacial maximum in mid-latitudes: Science (New York, N.Y.), v. 312, no. 5779, p. 1510–3, doi: 10.1126/science.1122872.

Thackray, G.D., 2008, Varied climatic and topographic influences on Late Pleistocene mountain glaciation in the western United States: Journal of Quaternary Science, v. 23, p. 671–681, doi: 10.1002/jqs.

Vanmarcke, E., 1983, Random Fields: Analysis and Synthesis: Cambridge, MA, MIT Press, 382 p.

Young, N.E., Briner, J.P., Leonard, E.M., Licciardi, J.M., and Lee, K., 2011, Assessing climatic and nonclimatic forcing of Pinedale glaciation and deglaciation in the western United States: Geology, v. 39, no. 2, p. 171–174, doi: 10.1130/G31527.

FIGURE CAPTIONS

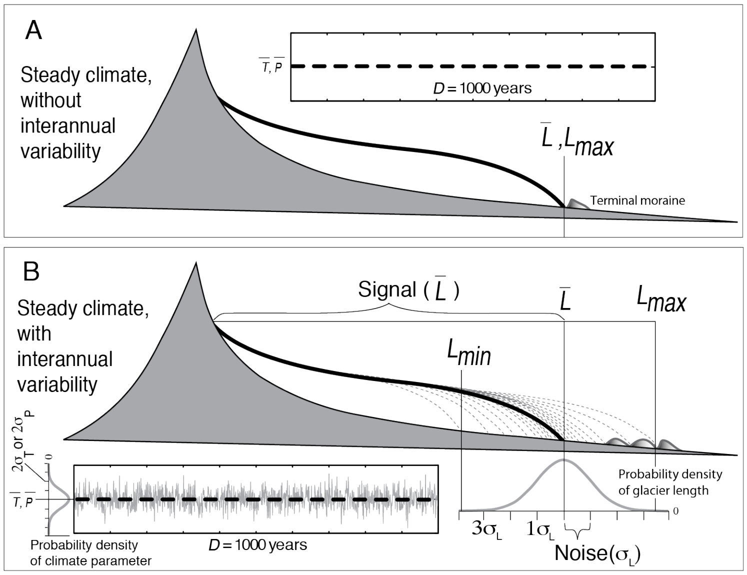

Figure 1. (A) A glacier forced only by $\overline{P}$ and $\overline{T}$ (bold dashed line) over time period, *D,* leads to a steady ice profile (bold black line) at $\overline{L}$. The maximum terminal moraine forms at $\overline{L}$. (B) A glacier forced by the same $\overline{P}$ and $\overline{T}$ as in A but with interannual variability included (grey white noise in the inset panel, which fills a normal distribution centered at $\overline{P}$ or $\overline{T}$) results in a terminus position that fluctuates around $\overline{L}$ and is shown by the grey dashed ice profiles. Given enough time, the terminus position fills a normal distribution centered at $\overline{L}$ (the signal; eq. 8) and is characterized by σ_L (the noise; eq. 7), the standard deviation of glacier length perturbations around $\overline{L}$. A change in $\overline{L}$ would occur with a change in $\overline{P}$ or $\overline{T}$ but not a change in σ_P or σ_T.

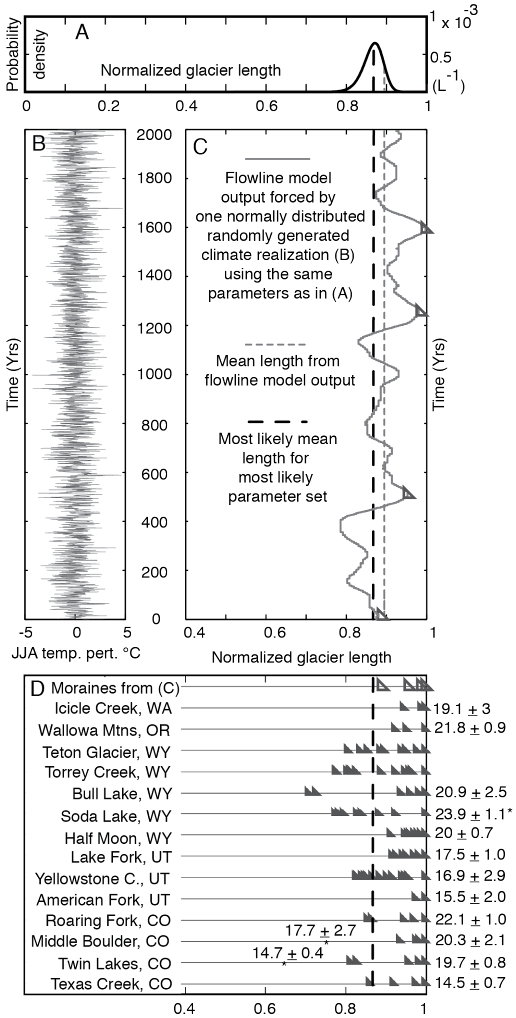

Figure 2. An illustration of the relationship between the mean glacier length and moraine formation. (A) The probability density function (pdf) of possible mean lengths derived from the most likely parameter set normalized by the maximum extent of the glacier. Eq. 8 gives the most likely mean length from this pdf. (B) An example melt-season climatology developed from a normally distributed random process, which is used to produce the example glacier terminus history in (C). (C) An example terminus history with potential moraine-forming locations indicated by triangles. The bold-dashed line is the most likely mean length from eq. 8. The grey

dashed line shows the mean length from the example terminus history derived from flowline model output using the same parameters as in (A). (D) Glacier length normalized to the LGM maximum terminal moraine with terminal moraines in-board from the maximum extent shown as triangles for western US LGM glacial valleys. Note the scatter in LGM maximum terminal moraines ages (ka) shown on the right (see supplemental for citations).

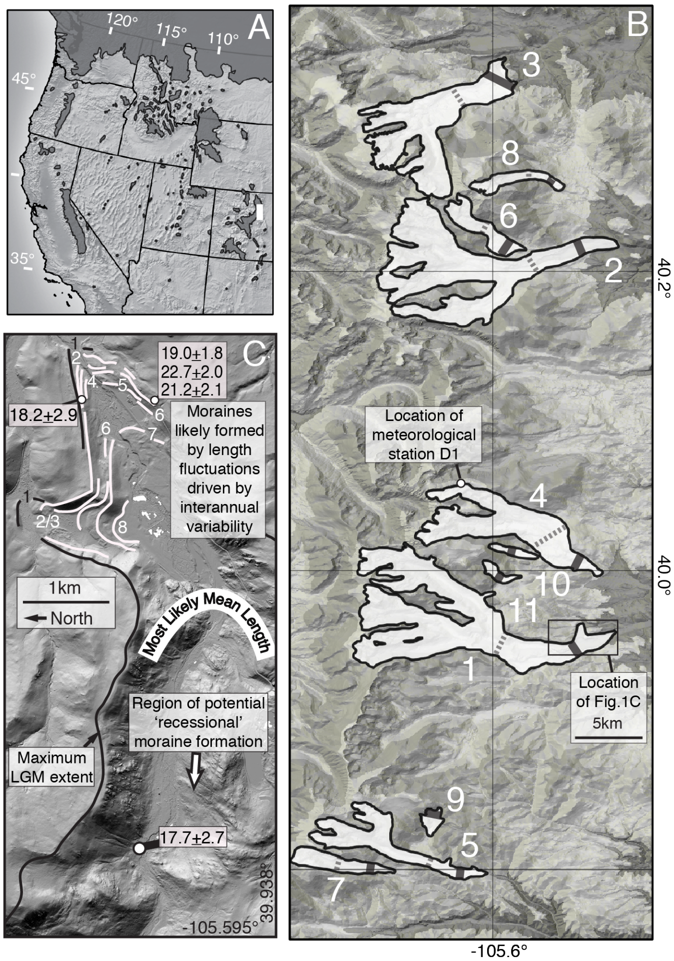

Figure 3. (A) Map of western US mountain glaciers during the LGM with generalized glacier outlines after Porter et al. (1983). (B) Shaded relief map showing the aerial extent of the eleven modeled glaciers (Table 2) and the location of the weather station used in this study. $\bar{L}_{mean}$, the most likely estimate of mean length, and $\bar{L}_{max}$, the maximum possible mean length, are shown for each modeled glacier. (C) LiDAR-derived hillshade of the terminal region of the LGM Middle Boulder Creek glacier. Cosmogenic radionuclide dates are in ka and are derived from Young et al. (2011) and references within. Numbers near moraines denote the number of distinct ice advances recorded in the pro-$\bar{L}$ area.

TABLE 1. LINEAR MODEL PARAMETERS AND GEOMETRY INPUTS

Name	Units	Description	Min.	Mean	Max.
μ	(m $^{\circ}$C^{-1} yr^{-1})	Melt factor	.5	.7	.9
Γ	($^{\circ}$C km^{-1})	On-ice near-surface lapse	3.5	5	6.5
AAR		Accumulation-area ratio	.5	.65	.8
$\overline{P}$	(m)	Mean annual precipitation	.6	1.2	2.4
σ_T	($^{\circ}$C)	Std. of summertime temp.	1	1.3	1.6
σ_P	(m a^{-1})	Std. of annual precipitation	.11	.22	.44
D	(yr)	Duration of climate change	500	4000	7500
Geometry Inputs					
A_{tot}		Total area of the glacier			
A_{abl}		Ablation area of the glacier			
$tan\phi$		Slope of the glacier bed			
w		Width of the ablation zone			
H		Thickness of the glacier			

TABLE 2. GLACIER GEOMETRY INPUTS, MEAN LENGTHS, AND SIGNAL-TO-NOISE RATIOS

Glacier name	Area (km^2)	Slope	Width (km)	Height (km)	L_{max} (km)	$\bar{L}_{min}$ % to L_{max}	Min Signal-to-Noise	$\bar{L}_{mean}$ % to L_{max}	Mean Signal-to-Noise	$\bar{L}_{max}$ % to L_{max}	Max Signal-to-Noise
1. Middle Boulder	56.62	0.031	1.30	0.22	18.5	0.97	40.22	0.86	16.68	0.62	5.09
2. North Saint Vrain	45.89	0.050	1.16	0.19	15.2	0.97	45.19	0.88	19.63	0.68	6.74
3. Bear Lake	31.19	0.055	1.56	0.16	12.6	0.97	43.11	0.87	17.70	0.63	5.28
4. North Boulder	26.00	0.091	1.32	0.11	12.4	0.97	52.51	0.89	22.94	0.71	8.03
5. Fall Creek	14.57	0.078	0.58	0.14	10.5	0.96	41.52	0.86	17.86	0.65	5.93
6. Hunter's Creek	6.25	0.138	0.81	0.09	6.19	0.96	39.80	0.85	16.12	0.59	4.56
7. Mill Creek	5.80	0.089	0.52	0.11	5.94	0.95	27.17	0.79	10.27	0.41	2.14
8. Roaring Fork	4.11	0.178	0.51	0.08	5.72	0.96	42.22	0.86	17.69	0.63	5.49
9. Silver Creek	1.67	0.131	0.45	0.04	2.07	0.83	7.51	0.28	1.11	-1.19	-1.72
10. Rainbow Creek	1.42	0.120	0.44	0.04	2.92	0.87	9.95	0.43	2.11	-0.77	-1.37
11. Horseshoe	1.41	0.137	0.35	0.05	2.86	0.90	13.24	0.57	3.64	-0.30	-0.74

*Signal-to-noise ratio $\equiv \bar{L}/\sigma_L$

[1]GSA Data Repository item 2013xxx, Sections DR.1-DR.5 are available online at www.geosociety.org/pubs/ft2009.htm, or on request from editing@geosociety.org or Documents Secretary, GSA, P.O. Box 9140, Boulder, CO 80301, USA.

The effects of interannual climate variability on the moraine record

Leif S. Anderson, Gerard H. Roe, and Robert S. Anderson

Section DR.1 On-ice near surface lapse rates

The selection of the lapse rate, Γ, for glaciological purposes must be made with care because reported summertime on-ice (≡ measurements only on the glacier surface), near-surface (≡ measurements made 2 m above the surface) lapse rates vary by nearly a factor of eight (Table A). Since Γ governs how ablation changes with elevation, much of the uncertainty in the results arises from this parameter. We argue that observed on-ice, summertime lapse rates provide a better approximation of the relevant paleo lapse rates than either the standard moist adiabatic lapse rate, observed free atmospheric lapse rates, or observed off-ice (measurements made off-glacier) near-surface lapse rates— even in those in the Front Range.

Lapse rates in the free atmosphere are determined by atmospheric vertical mixing and moisture. However, surface lapse rates are controlled surface radiative transfer and by the near surface environment (surface albedo, roughness, topographic aspect, and local meteorological effects)(e.g., Marshall and Sharp, 2007). While the use of modern summer near-surface temperature lapse rates from the Front Range is likely more appropriate than the often-used 6.5 °C km^{-1} moist adiabatic lapse rate, modern environmental conditions obviously differ greatly from likely summer conditions on an LGM glacier (presence of ice, reduced roughness, different elevation and topography due to the presence of the glacier). We therefore used modern on-ice near-surface temperature lapse rates to guide our uncertainty analysis. Table A shows that the most likely mean summer on-ice near surface lapse rate is 4.9 °C km^{-1} with a 1σ value of 1.7 °C km^{-1}. Extreme mean values are 1.1 °C km^{-1} (Pasterze Glacier, Austria) and 7.9 °C km^{-1} (Greenland Ice Sheet).

Table A. COMPILATION OF ON-ICE NEAR SURFACE LAPSE RATES

Valley Glaciers					
Location	Classification	Latitude	Lapse Rate °C km^{-1}	Period of Averaging	Reference
Pasterze Glacier, Austria	Valley	47°N	1.1	June, July	Greuell and Smeets, 2001
John Evans Glacier, Canada	Valley	80°N	1.1	Summer	Arendt and Sharp, 1999
Pasterze Glacier, Austria	Valley	47°N	1.4	June, July	Greuell and Smeets, 2001
Haut Glacier, Switzerland	Valley	45.97°N	2.0	Summer	Strasser et al., 2004
John Evans Glacier, Canada	Valley	80°N	3.1	Summer	Gardner et al., 2009
Pasterze Glacier, Austria	Valley	47°N	3.5	June, August	Denby and Greuell, 2000
Franz Josef Glacier, New Zealand	Valley	43.49°N	4.8	Annual	Anderson et al., 2006
Keqicar Glacier, Tien Shan	Valley	41.75°N	5.0	July	Li et al, 2011
South Glacier, Yukon	Valley	60.8°N	5.3	Annual	MacDougall and Flowers, 2011
Storglaciären, Sweden	Valley	67.9°N	5.5	Annual	Hock and Holmgren, 2005
North Glacier, Yukon	Valley	60.8°N	6.0	Annual	MacDougall and Flowers, 2011
Keqicar Baqi, Tien Shan, China*	Valley	41.75°N	6.0	Summer	Zhang et al., 2007*
South Cascade Glacier, WA	Valley	48.35°N	6.5	Summer	Anslow et al., 2008
Juncal Norte, Chile	Valley	32.6°S	6.5	Summer	Petersen and Pellicciotti, 2011
Miage glacier, Italy*	Valley	45.5°N	6.7	Summer	Brock et al., 2010*
Baltoro Glacier, Pakistan*	Valley	35.7°N	7.5	Summer	Mihalcea et al., 2006*
Miage glacier, Italy*	Valley	45.5°N	8.0	Summer	Brock et al., 2010*
	Valley Glacier Mean:		*4.7±2.2*	*w/ debris-cover*	

			4.0±2.1	*w/o debris-cover*	
Ice Sheet and Ice Cap					
Location	Classification	Latitude	Lapse Rate °C km^{-1}	Period of Averaging	Reference
Vatnajökull, Iceland	Ice Cap	64.1°N	3.6	Summer	Oerlemans et al., 1999
Prince of Whales Icefield, Canada	Ice Cap	78°N	3.7	JJA	Marshall et al., 2007
Prince of Whales Icefield, Canada	Ice Cap	78°N	4.3	Summer	Marshall et al., 2007
Prince of Wales Ice Field, Canada	Ice Cap	78°N	4.4	Summer	Marshall and Sharp, 2009
Prince of Whales Icefield, Canada	Ice Cap	78°N	4.6	Summer	Gardner et al., 2009
Devon Ice Cap, Canada	Ice Cap	75.2°N	4.8	Summer	Mair et al. 2005
Prince of Whales Icefield, Canada	Ice Cap	78°N	4.8	JJA	Marshall et al., 2007
Devon Ice Cap, Canada	Ice Cap	75.2°N	4.9	Summer	Gardner et al., 2009
Prince of Whales Icefield, Canada	Ice Cap	78°N	5.3	JJA	Marshall et al., 2007
Langjökull, Iceland	Ice Cap	64.5°N	5.6	JJA	Gudmundsson, et al, 2003
Vestari Hagafellsjökull, Iceland	Ice Cap	64.5°N	5.7	Summer	Hodgkins et al., 2012
King George Island, Antarctica	Ice Cap	62.3°S	6	Summer	Braun and Hock, 2004
Aggasiz Ice Cap, Canada	Ice Cap	80.2°N	6.4	Summer	Gardner et al., 2009
Greenland Ice Sheet (>1000m a.s.l)	Ice Sheet	~67°N	2.4	Summer	Oerlemans and Vugts, 1993
Greenland Ice Sheet	Ice Sheet	60-	4	June	Steffen and Box, 2001
NE Greenland Ice Sheet	Ice Sheet	70-	4	June, August	Boggild et al., 1994
Greenland Ice Sheet (<1000m a.s.l.)	Ice Sheet	60-	4.3	Summer	Hanna et al., 2005
Greenland Ice Sheet	Ice Sheet	60-	5	June, July	Box and Rinke, 2003
Greenland Ice Sheet (<1000m a.s.l.)	Ice Sheet	~67°N	5	Summer	Oerlemans and Vugts, 1993
West Greenland Ice Sheet	Ice Sheet	~67°N	5.8	Mean	van den Broeke et al., 2011
Greenland Ice Sheet (<1000m a.s.l.)	Ice Sheet	~67°N	6.3	Summer	Oerlemans and Vugts, 1993
West Greenland Ice Sheet	Ice Sheet	~67°N	7.4	Mean	van den Broeke et al., 2011
Greenland Ice Sheet (>1000m a.s.l.)	Ice Sheet	60-	7.9	Summer	Hanna et al., 2005
	Ice Sheet and Ice Cap Mean:		*5.1±1.2*		
* Debris-covered glacier	Mean of all cited lapse rates:		*4.9±1.7*	*w/ debris-cover*	
	Mean of all cited lapse rates:		*4.7±1.6*	*w/o debris-cover*	

Section DR.2 Melt-factors

The melt factor, μ, employed in our ablation parameterization is a simplified form of the often used positive-degree-day model that relates mean summer temperatures to vertical surface mass loss. The melt factor μ is converted from published positive-degree-day factors by assuming a melt season covering the months of June, July, and August (Table B). The selection of μ must be made with care as positive degree-day factors for snow can vary by nearly a factor of ten, and for ice by a factor of six. We combine and supplement several previous compilations of snow and ice melt-factors for modern glaciers and mountainous regions. Table B shows that the most likely positive degree day factor for ice: is 7.7 m °C^{-1} a^{-1} with a 1σ value of 3.2 m °C^{-1} a^{-1} with extreme values of 20 m °C^{-1} a^{-1}; Van de Wal (1992) and 2.6 m °C^{-1} a^{-1}; Zhang et al. (2006); and the most likely positive degree day factor for snow is 4.5 m °C^{-1} a^{-1} with a 1σ value of 1.7 m °C^{-1} a^{-1} with extreme values of 11.6 m °C^{-1} a^{-1}; Kayastha et al. (2000) and 1.4 m °C^{-1} a^{-1} Howat et al. (2007). It is important to note that our parameter combinations produce mass balance values that are reasonable for continental climates.

TABLE B. GLOBAL COMPILATION OF POSITIVE DEGREE-DAY MELT FACTORS

Greenland

Location	Snow	Ice	Elevation	Latitude	Duration	Reference	Cited in
Thule Ramp, Greenland		12	570	76°25'N	1 Jul - 31 Jul 1954	Schytt, 1955	Hock, 2003
Thule Ramp, Greenland		7	570		1 Aug-31 Aug 1954	Schytt, 1955	Hock, 2003
Camp IV-EGIG, Greenland		18.6	1013	69°40'N	Melt season 1959	Ambach, 1988a	Hock, 2003
GIMEX profile, Greenland		8.7	341	67°06'N	10 Jun-31 Jul 1991	Van de Wal, 1992	Hock, 2003
GIMEX profile, Greenland		9.2	519	67°06'N	15 Jun-6 Aug 1991	Van de Wal, 1992	Hock, 2003
GIMEX profile, Greenland		***20***	1028	67°04'N	15 Jun-6 Aug 1991	Van de Wal, 1992	Hock, 2003
Qamanârssûp sermia, Greenland	2.8	7.3	370-1410	64°28'N	1979-1987	Johannesson et al., 1995	Hock, 2003
Qamanârssûp sermia, Greenland	2.9	8.2	790	64°28'N	512 days (1980-86)	Braithwaite, 1995	Hock, 2003
Nordboglacier, Greenland	3.7	7.5	880	61°28'N	415 days (1979-83)	Braithwaite, 1995	Hock, 2003
Kronprins Christian Land, Greenland		9.8	380	79°54'N	8 Jul - 27 Jul 1999	Braithwaite et al., 1998	Hock, 2003
Hans Tausen Ice Cap, Greenland		5.9	540	82°49'N	2 Jul-5 Aug 1994	Braithwaite et al., 1998	Hock, 2003
Qamanârssûp sermia, Greenland	2.5	7.7	~800	64°28'N	Summer	Braithwaite, 1989	Braithwaite and Zhang, 2000
Qamanârssûp sermia, Greenland		7.9	790	64°28'N	May-Sep 1980-1986	Braithwaite, 1993	Braithwaite and Zhang, 2000
Greenland means:	*3.0±0.5*	*10.0±4.4*					

Europe/Americas/NZ

Location	Snow	Ice	Elevation	Latitude	Duration	Reference	Cited in
Aletshgletscher, Switzerland		11.7	2220	46°270' N	2 Aug - 27 Aug,1965	Lang, 1986	Hock, 2003
Ålfotbreen, Norway	4.5	6	850-1400	61°45'N	1961-1990	Laumann and Reeh, 1993	Hock, 2003
Ålfotbreen, Norway	3.5	5.5	1450-2200	61°34'N	1961-1990	Laumann and Reeh, 1993	Hock, 2003
Ålfotbreen, Norway	4	5.5	300-2000	61°41'N	1961-1990	Laumann and Reeh, 1993	Hock, 2003
Nigardsbreen, Norway	4.4	6.4	300-2000	61°41'N	1964-1990	Johannesson et al., 1995	Hock, 2003
Storglaciären, Sweden	3.2		1550	67°55'N	5 Jul-7 Sep 1993	Hock, 1999	Hock, 2003
Storglaciären, Sweden		6	1370	67°55'N	5 Aug - 12 Aug 1993	Hock, 1999	Hock, 2003
Storglaciären, Sweden		6.4	1370	67°55'N	19 Jul-27 Aug 1994	Hock, 1999	Hock, 2003
Storglaciären, Sweden		5.4	1250	67°55'N	9 Jul-4 Sep 1994	Hock, 1999	Hock, 2003
Vestfonna, Spitzbergen		13.8	310-410	~80°N	26 Jun - 5 Aug 1958	Schytt, 1964	Hock, 2003
Satujökull, Iceland	5.6	7.7	800-1800	~65°N	1987-1992	Johannesson et al., 1995	Hock, 2003
Aletshgletscher, Switzerland	5.3		3366	46°270' N	3 Aug-19 Aug, 1973	Lang, 1986	Hock, 2003
John Evans Glacier, Canada	5.5		260	79°40' N	27 Jun-29 Jun 1996	Arendt and Sharp, 1999	Hock, 2003
John Evans Glacier, Canada	4.1		820	79°40' N	19 Jun - 14 Jul 1996	Arendt and Sharp, 1999	Hock, 2003
John Evans Glacier, Canada	3.9		820	79°40' N	23 May - 1 Jul 1998	Arendt and Sharp, 1999	Hock, 2003
John Evans Glacier, Canada	3.9		1180	79°40' N	25 Jun-19 Jul 1996	Arendt and Sharp, 1999	Hock, 2003
John Evans Glacier, Canada	2.7		1180	79°40' N	31 May - 19 Jul 1996	Arendt and Sharp, 1999	Hock, 2003
John Evans Glacier, Canada		7.6	260	79°40' N	4 Jul - 16 Jul 1996	Arendt and Sharp, 1999	Hock, 2003
John Evans Glacier, Canada		8.1	820	79°40' N	15 Jul - 19 Jul 1996	Arendt and Sharp, 1999	Hock, 2003
John Evans Glacier, Canada		5.5	820	79°40' N	2 Jul -19 Jul 1998	Arendt and Sharp, 1999	Hock, 2003
Weissfluhjoch, Switzerland	4.2		2540	46°48'N	28 year record	de Quervain, 1979	Braithwaite and Zhang, 2000
Franz Josef Glacier, New Zealand	3	6	122	43°28'N	Summer	Woo and Fitzharris, 1992	Braithwaite and Zhang, 2000
Saint Supphellebreen, Norway		6.3		61°30'N	Summer	Orheim, 1970	Braithwaite and Zhang, 2000
Glacier de Sarennes, France	3.8	6.2	~3000	45°10'N	Summer	Vincent and Vallon, 1997	Braithwaite and Zhang, 2000
Griesgletscher, Switzerland		8.9	2287	46°39'N	112 summer days	Braithwaite, 2000	Braithwaite and Zhang, 2000
Australian Alps	2.9		1250	36°30'S	1966-1985	Whetton, et al., 1996	Brugger, 2010
Blöndujökull, Kv́ ıslajökull, Iceland	4.5	5	115	64°50'N	Summer	Johennesson, 1997	Brugger, 2010
Illvirajökull, Iceland	5.6	7.6	115	64°50'N	Summer	Johennesson, 1997	Brugger, 2010
Glacier Upsala, Patagonia		7.1	350	49°58S	Summer 1993-1994	Naruse et al., 1997	Brugger, 2010
South Cascade Glacier, USA		6.2	1980	48°21'N	Summer	Tangborn,1999	Brugger, 2010
Rabots Glacier, Sweden	4.7	6.8	~1300	67°55'N	Summer	Refsnider, 2001	Brugger, 2010
Sverdrup Glacier, Canada		4	300	75°N	Summer 1963	Braithwaite, 1981	

Andrews Glacier, USA	4.3				Summer	Outcalt and MacPhail, 1965	Lauman & Reeh, 1993
Storsteinsfjellbreen, Norway	5,6	7.5		68°15'N	Summer	Pytte and Liestol, 1966	Lauman & Reeh, 1993
Storbreen, Norway		5.5		61°34'N	Summer 1949-1965	Liestol, 1967	Lauman & Reeh, 1993
White Glacier, Canada		4.9	210	79°N	Summer 1960-1962	Braithwaite, 1981	
Alfotbreen, Norway	5.3	7.5		61°45'N	Summer 1965	NVE, 1965	Lauman & Reeh, 1993
Various Swiss glaciers		6		~46°30'N	Summer	Kasser, 1959	Braithwaite and Zhang, 2000
Fillefjell, Norway	3.9			61°10'N	Summer 1967-1964	Furmyr and Tollan, 1975	Lauman & Reeh, 1993
Moreno glacier, Argentina		7	330	50°28'S	1993 -1994	Takeuchi et al., 1996	Hock, 2003
Martial Este Glacier, Argentina	4.7	9.4	990	54°47'S	Dec 2005 - Feb 2006	Buttstadt et al., 2009	
Haut Glacier d'Arolla, Switzerland	7.7	10.8	~2900	45°58'N	May - Sep 2001	Pellicciotti et al., 2005	
Mount Shasta, Cascade Range, USA	1.6	6.9	2600	41°12'N	May - Nov 2002	Howat et al., 2007	
Mount Shasta, Cascade Range, USA	***1.4***	5.5	3000	41°12'N	May - Nov 2002	Howat et al., 2007	
Hansbreen, Svalbard	6	8.3	180	77°05'N	JJA, 2008	Grabiec et al., 2012	
Franz Josef Glacier, New Zealand	4.6	7.1		43°28'N	Summer	Anderson, 2004	
Hansbreen, Svalbard		6.8	316	77°05'N	1994-1995	Szafraniec, 2002	
Gran Campo Nevado Ice Cap, Chile		7.6	450	53°S	Feb - Apr 2000	Schneider et al., 2007	
Tasman Glacier, New Zealand		4.5	1360	43°37'S	1985-1986	Kirkbride, 1995	
Tasman Glacier, New Zealand		5	1360	43°37'S	1986-1987	Kirkbride, 1995	
Tasman Glacier, New Zealand		3.9	960	43°37'S	1985-1986	Kirkbride, 1995	
Tasman Glacier, New Zealand		3.6	960	43°37'S	1986-1987	Kirkbride, 1995	
Glacier de Saint-Sorlin, France	4	6.4	2760	45°N	21 Jul- 31 Jul 2006	Six et al., 2009	
Koryto Glacier, Kamchatk, Russia	4.7	7	810	54°50'N	7 Aug-12 S. 2000	Konya et al., 2004	
Europe/America/NZ means:	*4.3±1.3*	*6.8±2.0*					
Central Asia							
Location	Snow	Ice	Elevation	Latitude	Duration	Reference	Cited in
Urumqi glacier,Tien Shan, China	6.3	8.5	3831-3945	~42°N	1986-1993	Liu et al., 1996	Zhang_etal 2006
Urumqui glacier,Tien Shan, China		7.3	3754-3898	~42°N	1986-1988	Liu et al., 1996	Zhang_etal 2006
Urumqui glacier,Tien Shan, China	3.1		4048	~42°N	1986-1993	Liu et al., 1996	Zhang_etal 2006
Keqicar Baqi, Tien Shan, China		4.5	3347	~42°N	28 Jun- 12 Sep 2003	Zhang et al., 2005	Zhang_etal 2006
Keqicar Baqi, Tien Shan, China		7	4216	~42°N	11 Jul-13 Sep 2003	Zhang et al., 2005	Zhang_etal 2006
Qiongtailan glacier, Tien Shan, China		4.5	3675	~42°N	17 Jun- 14 Aug 1978	Zhang et al., 2006	
Qiongtailan glacier, Tien Shan, China		7.3	4100	~42°N	25 Jun-14 Aug 1978	Zhang et al., 2006	
Qiongtailan glacier, Tien Shan, China		8.6	4200	~42°N	21 Jun-31 Jul 1978	Zhang et al., 2006	
Qiongtailan glacier, Tien Shan, China	3.4		4400	~42°N	21 Jun- 11 Aug 1978	Zhang et al., 2006	
Hailuogou, Hengduan mtns, China		5	3301	~30°N	Aug 1982- Aug 1983	Zhang et al., 2006	
Baishuihe Hengduan mtns, China		13.3	4600	~30°N	23 Jun- 30 Aug 1982	Zhang et al., 2006	
Baishuihe,Hengduan mtns, China	5.9		4800	~30°N	26 Jun- 11 Jul 1982	Zhang et al., 2006	
Dagongba glacier, Hengduan, China		13.2	4540	~30°N	Sep 1982- Sep 1983	Zhang et al., 2006	
Xiaogongba glacier, China		12	4550	~30°N	Jul 1982- Jul 1983	Zhang et al., 2006	
Batura, Karakoram, China		3.4	2780	~36°N	Jun-Aug 1975	Zhang et al., 2006	
Teram Kangri, Karakoram, China		5.9	4630	~36°N	25 Jun- 7 Sep 1987	Zhang et al., 2006	
Teram Kangri, Karakoram, China		6.4	4650	~36°N	24 Jun- 7 Sep 1987	Zhang et al., 2006	
Qirbulake, Karakoram, China		***2.6***	4750	~36°N	6 Jun- 30 Jul 1960	Zhang et al., 2006	
Yangbulake, Karakoram, China		4.3	4800	~36°N	1Jul - 5 Jul 1987	Zhang et al., 2006	
Meikuang, Kunlun Shan, China		3	4840	~36°N	7 May- Sep 1989	Zhang et al., 2006	
Halong, Kunlun Shan, China		4.7	4616	~36°N	15 Jun- 28 Jun 1981	Zhang et al., 2006	
Halong, Kunlun Shan, China		3.6	4900	~36°N	14 Jun 27 Jun 1981	Zhang et al., 2006	
Xiaodongkemadi, Tanggula, China		13.8	5425-5475	~32°30'N	Jul- Aug 1993	Kayastha et al., 2003	Zhang_et al., 2006
Qiyi, Qilian Shan, China		7.2	4305-4619	~39°N	Jul- Aug 2002	Kayastha et al., 2003	Zhang_et al., 2006
Kangwure, Himalaya, China		9	5700-6000		20 Jul-25 Aug 1993	Zhang et al., 2006	
Urumqi Glacier, Tien shan, China	5.2	8.4		~42°N	Summer	Cui, 2009	Xianzhong, et al., 2010

Urumqi Glacier, Tien shan, China	3.1	7.1		~42°N	Summer	Cui, 2009	Xianzhong, et al., 2010
Urumqi Glacier, Tien shan, China	5.2	7.1		~42°N	Summer	Cui, 2009	Xianzhong, et al., 2010
Urumqi Glacier, Tien shan, China		4		~42°N	Summer	Cui, 2009	Xianzhong, et al., 2010
Baishui Glacier, Hengduan, China		4.92	4200	26°00'N	26 Jun-11 Jul 1982	Liu, 1996	Xianzhong, et al., 2010
Baishui Glacier, Hengduan, China		10.3	4600	26°00'N	Sept 2008	Xianzhong, et al., 2010	
Baishui Glacier, Hengduan, China		13.6	4700	26°00'N	Sept 2008	Xianzhong, et al., 2010	
Baishui Glacier, Hengduan, China		14.1	4800	26°00'N	Sept 2008	Xianzhong, et al., 2010	
Baishui Glacier, Hengduan, China	2.4		4400	26°00'N	13 May-6 Jun 2009	Xianzhong, et al., 2010	
Baishui Glacier, Hengduan, China	2.8		4500	26°00'N	13 May-6 Jun 2009	Xianzhong, et al., 2010	
Baishui Glacier, Hengduan, China	4.6		4600	26°00'N	5 May - 6 Jun 2009	Xianzhong, et al., 2010	
Baishui Glacier, Hengduan, China	5.2		4700	26°00'N	13 May-6 Jun 2009	Xianzhong, et al., 2010	
Baishui Glacier, Hengduan, China	5.8		4800	26°00'N	13 May - 6 Jun 2009	Xianzhong, et al., 2010	
Dokriani Glacier, Himalaya	5.9		4000	31°45' N	4 Jun-6Jun 1995	Singh and Kumar, 1996	Hock, 2003
Dokriani Glacier, Himalaya	5.7	7.4	4000	31°45' N	4 days (1997-98)	Singh et al., 2000a,b	Hock, 2003
Glacier AX010, Himalaya	7.3	8.1	4956	27°45' N	Jun-Aug 1978	Kayastha et al., 2000a	Hock, 2003
Glacier AX010, Himalaya	8.7	8.8	5072	27°45' N	Jun-Aug 1978	Kayastha et al., 2000a	Hock, 2003
Glacier AX010, Himalaya	***11.6***		5245	27°45' N	1 Jun-31 Aug 1978	Kayastha et al., 2000a	Hock, 2003
Khumbu Glacier, Himalaya		16.9	5350	28°00'N	21 May-1 Jun 1999	Kayastha et al., 2000b	Hock, 2003
Rakhiot Glacier, Himalaya		6.6	3350	35°22'N	18 Jul-6 Aug 1986	Kayastha et al., 2000b	Hock, 2003
Yala Glacier, Himalaya		9.3	5120	28°14'N	1 Jun-31 Jul 1996	Kayastha, 2001	Hock, 2003
Yala Glacier, Himalaya		10.1	5270	28°14'N	1 Jun-31 Jul 1996	Kayastha, 2001	Hock, 2003
Central Asia means:	*5.4±2.3*	*7.9±3.6*					
Non-glaciated Sites							
Location	Snow	Ice	Elevation	Latitude	Duration	Reference	Cited in
Gooseberry Creek, Utah, USA	2.5		2650	~38°N	23 Apr-9 May 1928	Clyde, 1931	Hock, 2003
Weissfluhjoch, Switzerland	4.5		2540	46°48'N	Snowmelt season	Zingg, 1951	Hock, 2003
3 basins in USA	2.7				Several seasons	C. of Engineers, 1956	Hock, 2003
3 basins in USA	4.9				Several seasons	C. of Engineers, 1956	Hock, 2003
Former European USSR	5.5	7	1800-3700			Kuzmin, 1961, p. 117	Hock, 2003
12 sites in Finland	3.9			~60-68°N	1959-1978	Kuusisto, 1980	Hock, 2003
Non-glaciated site means:	*4.0±1.2*	*7.0*					
Mean meltfactor for all examples in the literature:	***4.5±1.7***	***7.7±3.2***					

Section DR.3 Discussion of terminal moraine assumptions

In order to support our assumption that terminal moraines can form during advances driven by interannual variability without long term terminus standstills (< 20 years; a time scale supported by flowline modeling (see Roe, 2011 Figure 4)), we present a review of the moraine sedimentological literature (Table C), which shows that the majority of moraines with constrained formation periods form over periods less than 20 years. The development of a universal model for the timescale of moraine formation has been hampered by the complexity of formational processes, the abundance of unconstrainable variables and initial conditions. The length of time needed to form terminal moraines is dependent on the process of formation and can be constrained only crudely. Ice marginal indicators are typically divided into glaciotectonic, push, hummocky, drop moraines, and ice-contact fans but composite moraines are common (Benn and Evans, 1998). For the purposes of justifying the short timescale of ice marginal deposit formation (<20 years), we further divide the indicators into those that are independent of terminus standstills (glaciotectonic, push and hummocky moraines) and those that are dependent on terminus standstills (drop moraines and ice-contact fans).

TABLE C. COMPILATION OF MORAINE FORMATION TIMES

Region	Time period	Type	Sub-Category	Time of formation	Height	Reference
Iceland	Modern	Push	Imbricate	1 year	3-5m	Humlum, 1985
Iceland	Modern	Push	Lodgement freeze on	Seasonal	.3 -.7m	Krüger, J., 1995
Iceland	LIA	Push	Fold and thrust	2-6 days		Benediktsson et al., 2010
Iceland	LIA	Push	Fold and thrust	12yrs at terminus		Bennett et al., 2000
Iceland	LIA	Push	Single large nappe and faulting	<39 likely 1 or 2 yrs	8m	Bennett et al., 2004
Iceland	Modern	Push		Seasonal	1-2m	Boulton, 1986
Norway	LIA and modern	Push	Bulldozing and thrusting	1-10years	3-8m	Burki et al., 2009
Iceland	Modern	Push	Polygenetic push	Seasonal	.4-5.25m	Sharp, 1984
Argentina	Modern	Push		1 year	2.5m	Rabassa et al., 1979
Iceland	LIA	Push/Thrust	1890 Surge	1 day	5m	Benediktsson et al., 2008
Scotland	Younger Dryas	Ice Contact Fan and push	Debris flow and alluvium	3-9 or 7-19 years		Benn and Lukas, 2006
Rocky Mtns	LGM	Ice Contact Fan	Debris flow and alluvium	<20 years		Johnson and Gillham, 1995
Iceland	Modern	Ice Contact Fan	Glaciofluvial outwash fans/ sandar	<10years	<10m	Boulton, 1986
Iceland	Modern	Ice Contact Fan then push	Glacier is oscillating seasonally	<21yrs		Boulton, 1986
Patagonia	Modern	Ice cored/ Push	Folding and Thrusting	<13 years	15-20m	Glasser and Hambrey, 2002
Alaska	Modern	Ice Cored/ Push	Readvance in a Surging glacier	1 year	3m	Johnson, 1972
Svalbard	LIA	Ice Cored	Retreating from LIA maximum	Formed upon retreat	25-30m	Lyså and Lønne, 2001
Svalbard	Neoglacial	Thrust	Melt out thrust	Formed upon retreat	<20m	Bennett et al., 1996
Iceland	Modern	Dump	Minor push component	<20 years	4-7m	Krüger et al., 2002
Iceland	Modern	Basal Freezing		1 year	1.5-2.5m	Krüger, 1993

Moraines independent of glacial standstills

The most rapidly forming moraines require the propagation of debris in front of an advancing ice front (e.g. Krüger, 1995; Benediktsson, et al., 2010; Benediktsson et al., 2008; Boulton, 1986; Humlum, 1985). Because the material is bulldozed or thrust in front of the glacier, the moraine can form during any advance and retreat cycle irrespective of time spent in standstill. The formation of glaciotectonic and push moraines is more dependent on the availability of sediment or permafrost in the foreland than it is on the glaciological conditions (Bennett, 2001). *Glaciotectonic Moraines* are formed when the stress imposed by an advancing glacier excavates and elevates (associated with thrusting and folding) proglacial bedrock and/or quaternary sediments. *Push Moraines* are formed by the bulldozing of proglacial sediment and typically have steep proximal and gentle distal slopes. Advances over long distances can result in formation of a more extensive set of moraine ridges. *Hummocky and ice-cored moraines* form when heavily debris-covered ice is dynamically separated from an active, retreating glacier (Lyså and Lonne, 2001). As these moraines are in place as soon as the ice is dynamically separated from the active glacier, all that remains is for the ice core to waste away. Ice-cored and hummocky moraines do not require a glacial standstill to form (Glassner and Hambrey, 2002; Johnson, 1972) and their identification in the moraine record implies that the moraine was emplaced instantaneously for the timescales of interest for this study.

Moraines dependent on glacial standstills
Latero-frontal fans and dump moraine sizes are dependent on the debris flux off the glacier and the length of time the glacier terminus remains stationary. A glacier that advances and retreats without a terminus standstill will not likely form an ice-contact fan or a dump moraine, although there are reported occurrences in the literature. One of these potential influences is thick supraglacial debris-cover, which can slow terminus oscillations and provide the debris fluxes to create large moraines. *Ice-contact fans* form by the coalescence of debris fans and glaciofluvial processes at the glacier terminus. Although latero-frontal fans can form over short periods and even in a single short-lived advance, these fans are typically on the order 10 meters in height whereas fans that limit subsequent ice advances are typically 100s of meters in height (Benn and Lukas, 2006; Benn and Evans, 1998). *Dump Moraines* are formed by the delivery of supraglacial material derived from rockfall onto the glacier or the melt out of basal debris septa that flows or falls off the terminal ice slope. Paleoglacier valleys with large ice-contact fans (>100 m in height) or dump moraines should be treated with more caution than moraines that are independent of glacial standstills. Nearly all documented terminal moraine formation durations are less than 20 years (Table C). Further sedimentological and stratagraphic investigation of LGM terminal moraines is needed to constrain the importance of moraine formation timescale on paleoclimate reconstruction (e.g., Johnson and Gillam, 1995).

Terminal moraines do not limit subsequent advances
We have assumed that the furthest length excursion from the mean glacier length forms the maximum terminal moraine. In effect, this requires that that previously formed moraines do not limit the extent of subsequent advances. The only moraine types that have been shown to limit subsequent advances are large latero-frontal moraines or scree aprons; these are common in tectonically active regions such as the Himalaya, the Andes, and the New Zealand Alps. These moraines can become sufficiently massive to dam glacier ice and cause subsequent glacial advances to terminate at the same location (Lliboutry, 1977; Thorarinsson, 1956). This effect is especially apparent where large lateral moraines are deposited outside of cirques and steep valleys and are therefore less susceptible to paraglacial processes (Thorarinsson, 1956). Cases where latero-terminal moraines could have limited ice extent are easily identifiable by the height and extent of the latero-frontal moraines. These situations are unlikely to be found in LGM terminal moraines in the Western US.

Overridden terminal moraines are destroyed
Moraines can be overrun by subsequent advances and still be identifiable upon retreat (Karlén, 1973; Bennett et al., 2000). Overrun moraines may be differentiated from moraines that haven't been overrun by their subdued topography compared to moraines down valley, the presence of

fluted till overriding the moraine, and the presence of lateral continuations of the moraine that have not been overridden that exhibit a sharper morphology (Karlén, 1973). Preservation of overrun moraines is rare and the potential for preservation depends on the local bedrock topography and the amount of time the overrun moraine is subjected to subglacial processes. An overrun moraine could potentially pose a problem for paleoclimatic or mean glacial length reconstruction only if a moraine is overrun and there is no indication of the maximum extent of the overriding glacier. The overrun moraine would then be interpreted as the maximum extent of the glacier for the time period of interest and could produce substantial error. This situation is unlikely for LGM moraines, as any overrun moraine would have been smoothed by the overriding glacier and then subjected to at least 10 thousand years of diffusional surface process that would further obliterate the morainal form.

Section DR 4. LGM moraine complexes

LGM 'terminal moraines' in the western US are often composed of a conglomeration of moraines formed during numerous glacier advances. We call these clusters of moraines, terminal moraine complexes keeping in mind that it is possible that these clusters of ridges were formed by a single advance and the individual moraines interpreted as terminal moraines are actually fault bend folds from a glaciotectonic push moraine. Below in figure B we present a LiDAR hillshade of the Teton Glacier LGM terminal moraine and our interpretation of distinct terminal moraines and the subjective limits of the terminal moraine complex. This hillshade allows us to define many more ice marginal features than possible without detailed field surveys. The terminal moraines defined in figure B are likely formed between the LGM mean length and the maximum terminal moraine (labeled 1) and are therefore likely candidates for moraines formed by glacier length fluctuations driven by interannual variability.

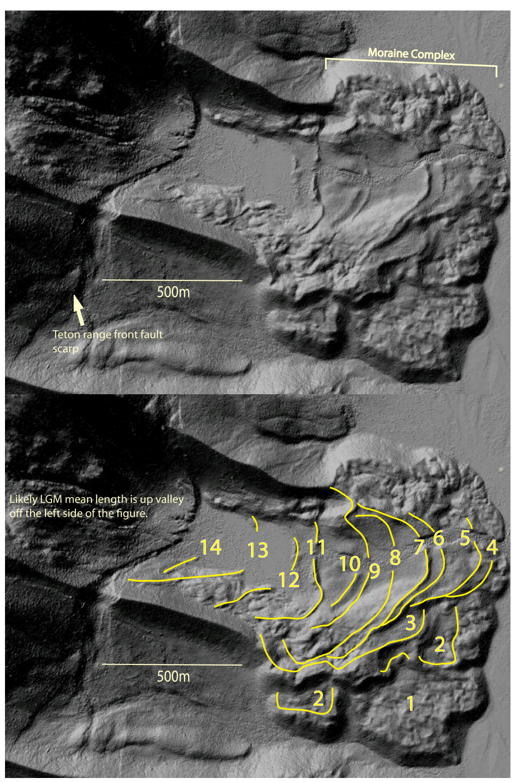

Figure A. LiDAR of the LGM Teton glacier terminal moraines. In the bottom panel we show what we interpret to be 14 distinct ice margins revealed by the LiDAR. The LiDAR is courtesy of OpenTopography.

DR.5 Relative sensitivity of length fluctuations due to temperature and precipitation variability

Roe and O'Neal (2009) show that the relative sensitivity of a glacier's fluctuations to temperature vs. precipitation variability is given by:

$$R = \frac{A_{T>0}\mu\sigma_T}{A_{Tot}\sigma_P}.$$

The R values for Front Range glaciers greater than 6 km^2 range between 2.2 and 2.9 with a mean of 2.5, suggesting that year-to-year variations in summer temperature were two to three times as important for driving length perturbations as were variations in annual precipitation. This dominant sensitivity to summertime temperature variation is expected in continental climates.

References for supplementary material

Anderson, B.M., 2004, The response of "Ka Roimata o Hine Hukatere" Franz Josef Glacier to climate change [Ph.D. Thesis]: Christchurch, University of Canterbury, 106 p.

Anderson, B.M., Lawson, W., Owens, I., and Goodsell, B., 2006, Past and future mass balance of "Ka Roimata o Hine Hukatere" Franz Josef Glacier, New Zealand: Journal of Glaciology, v. 52, no. 179, p. 597–607, doi: 10.3189/172756506781828449.

Anslow, F.S., Hostetler, S., Bidlake, W.R., and Clark, P.U., 2008, Distributed energy balance modeling of South Cascade Glacier, Washington and assessment of model uncertainty: Journal of Geophysical Research, v. 113, no. F2, p. F02019, doi: 10.1029/2007JF000850.

Arendt, A., and Sharp, M., 1999, Energy balance measurements on a Canadian high arctic glacier and their implications for mass balance modelling: IAHS Publication, 165-172.

Benediktsson, Í.Ö., Möller, P., Ingólfsson, Ó., Van der Meer, J.J.M., Kjær, K.H., and Krüger, J., 2008, Instantaneous end moraine and sediment wedge formation during the 1890 glacier surge of Brúarjökull, Iceland: Quaternary Science Reviews, v. 27, no. 3-4, p. 209–234, doi: 10.1016/j.quascirev.2007.10.007.

Benediktsson, Í.Ö., Schomacker, A., Lokrantz, H., and Ingólfsson, Ó., 2010, The 1890 surge end moraine at Eyjabakkajökull, Iceland: a re-assessment of a classic glaciotectonic locality: Quaternary Science Reviews, v. 29, no. 3-4, p. 484–506, doi: 10.1016/j.quascirev.2009.10.004.

Benn, D. I., and Evans, D. J., 1998, Glaciers and glaciation: London. Edward Arnold. 734 p.

Benn, D.I., and Lukas, S., 2006, Younger Dryas glacial landsystems in North West Scotland: an assessment of modern analogues and palaeoclimatic implications: Quaternary Science Reviews, v. 25, no. 17-18, p. 2390–2408, doi: 10.1016/j.quascirev.2006.02.015.

Bennett, M.R., 2001, The morphology, structural evolution and significance of push moraines: Earth-Science Reviews, v. 53, no. 3-4, p. 197–236, doi: 10.1016/S0012-8252(00)00039-8.

Bennett, M., Huddart, D., Hambrey, M.J., and Ghienne, J.F., 1996, Moraine development at the high-arctic valley glacier Pedersenbreen, Svalbard: Geografiska Annaler. Series A, v. 78, no. 4, p. 209–222.

Bennett, M.R., Huddart, D., and McCormick, T., 2000, An integrated approach to the study of glaciolacustrine landforms and sediments: a case study from Hagavatn, Iceland: Quaternary Science Reviews, v. 19, no. 7, p. 633–665, doi: 10.1016/S0277-3791(99)00013-X.

Bennett, M., Huddart, D., Waller, R., Cassidy, N., Tomio, a, Zukowskyj, P., Midgley, N., Cook, S., Gonzalez, S., and Glasser, N., 2004, Sedimentary and tectonic architecture of a large push moraine: a case study from Hagafellsjökull-Eystri, Iceland: Sedimentary Geology, v. 172, no. 3-4, p. 269–292, doi: 10.1016/j.sedgeo.2004.10.002.

Benson, L., Madole, R., Landis, G., and Gosse, J., 2005, New data for Late Pleistocene Pinedale alpine glaciation from southwestern Colorado: Quaternary Science Reviews, v. 24, no. 1-2, p. 49–65, doi: 10.1016/j.quascirev.2004.07.018.

Boulton, G., 1986, Push-moraines and glacier-contact fans in marine and terrestrial environments: Sedimentology, v. 33, p. 677–698.

Box, J., and Rinke, A., 2003, Evaluation of Greenland ice sheet surface climate in the HIRHAM regional climate model using automatic weather station data: Journal of Climate, v. 16, p. 1302–1319.

Braithwaite, R.J., 1981, On glacier energy balance, ablation, and air temperature. Journal of Glaciology, v. 27, p. 381–391.

Braithwaite, R.J., and Zhang, Y., 2000, Sensitivity of mass balance of five Swiss glaciers to temperature changes assessed by tuning a degree-day model: Journal of Glaciology, v. 46, no. 152, p. 7–14.

Braun, M., and Hock, R., 2004, Spatially distributed surface energy balance and ablation modelling on the ice cap of King George Island (Antarctica): Global and Planetary Change, v. 42, no. 1-4, p. 45–58, doi: 10.1016/j.gloplacha.2003.11.010.

Brock, B.W., Mihalcea, C., Kirkbride, M.P., Diolaiuti, G., Cutler, M.E.J., and Smiraglia, C., 2010, Meteorology and surface energy fluxes in the 2005–2007 ablation seasons at the Miage debris-covered glacier, Mont Blanc Massif, Italian Alps: Journal of Geophysical Research, v. 115, no. D9, p. D09106, doi: 10.1029/2009JD013224.

Brugger, K.A., 2010, Climate in the Southern Sawatch Range and Elk Mountains, Colorado, U.S.A., during the Last Glacial Maximum: Inferences using a simple degree-day model: Arctic, Antarctic, and Alpine Research, v. 42, no. 2, p. 164–178, doi: 10.1657/1938-4246-42.2.164.

Brugger, K.A., 2007, Cosmogenic ^{10}Be and ^{36}Cl ages from Late Pleistocene terminal moraine complexes in the Taylor River drainage basin, central Colorado, USA: Quaternary Science Reviews, v. 26, no. 3-4, p. 494–499, doi: 10.1016/j.quascirev.2006.09.006.

Burki, V., Larsen, E., Fredin, O., and Margreth, A., 2009, The formation of sawtooth moraine ridges in Bødalen, western Norway: Geomorphology, v. 105, no. 3-4, p. 182–192, doi: 10.1016/j.geomorph.2008.06.016.

Buttstadt, M., Moller, M., Iturraspe, R., and Schneider, C., 2009, Mass balance evolution of Martial Este Glacier , Tierra del Fuego (Argentina) for the period 1960 – 2099: Advances in Geosciences, v. 22, p. 117–124.

Bøggild, C., Reeh, N., and Oerter, H., 1994, Modelling ablation and mass-balance sensitivity to climate change of Storstrømmen, northeast Greenland: Global and Planetary Change, v. 9, p. 79–90.

Denby, B., and Greuell, W., 2000, The use of bulk and profile methods for determining surface heat fluxes in the presence of glacier winds: Journal of Glaciology, v. 46, no. 154, p. 445–452, doi: 10.3189/172756500781833124.

Gardner, A.S., Sharp, M.J., Koerner, R.M., Labine, C., Boon, S., Marshall, S.J., Burgess, D.O., and Lewis, D., 2009, Near-surface temperature lapse rates over Arctic glaciers and their implications for temperature downscaling: Journal of Climate, v. 22, no. 16, p. 4281–4298, doi: 10.1175/2009JCLI2845.1.

Glasser, N.F., and Hambrey, M.J., 2002, Sedimentary facies and landform genesis at a temperate outlet glacier: Soler Glacier, North Patagonian Icefield: Sedimentology, v. 49, no. 1, p. 43–64, doi: 10.1046/j.1365-3091.2002.00431.x.

Gosse, J.C., Klein, J., Lawn, B., Middleton, R., and Evenson, E.B., 1995, Beryllium-10 dating of the duration and retreat of the last Pinedale glacial sequence: Science (New York, N.Y.), v. 268, no. 5215, p. 1329–33, doi: 10.1126/science.268.5215.1329.

Grabiec, M., Budzik, T., and Głowacki, P., 2012, Modeling and hindcasting of the mass balance of Werenskioldbreen (Southern Svalbard): Arctic, Antarctic, and Alpine Research, v. 44, no. 2, p. 164–179.

Greuell, W., and Smeets, P., 2001, Variations with elevation in the surface energy balance on the Pasterze (Austria): Journal of Geophysical Research, v. 106, no. D23, p. 31717–31727.

Guðmundsson, S., Björnsson, H., Palsson, F., and Haraldsson, H.H., 2003, Physical energy balance and degree-day models of summer ablation on Langjökull ice cap, SW-Iceland: National Power Company of Iceland.

Hanna, E., Huybrechts, P., Janssens, I., Cappelen, J., Steffen, K., and Stephens, A., 2005, Runoff and mass balance of the Greenland ice sheet: 1958–2003: Journal of Geophysical Research, v. 110, no. D13, p. D13108, doi: 10.1029/2004JD005641.

He, X., Du, J., Ji, Y., Zhang, N., Li, Z., Wang, S., and Theakstone, W.H., 2010, Characteristics of DDF at Baishui Glacier No. 1 region in Yulong Snow Mountain: Journal of Earth Science, v. 21, no. 2, p. 148–156, doi: 10.1007/s12583-010-0013-4.

Hock, R., 2003, Temperature index melt modelling in mountain areas: Journal of Hydrology, v. 282, no. 1-4, p. 104–115, doi: 10.1016/S0022-1694(03)00257-9.

Hock, R., and Holmgren, B., 2005, A distributed surface energy-balance model for complex topography and its application to Storglaciären, Sweden: Journal of Glaciology, v. 51, no. 172, p. 25–36.

Hodgkins, R., Carr, S., Pálsson, F., Guðmundsson, S., and Björnsson, H., 2013, Modelling variable glacier lapse rates using ERA-Interim reanalysis climatology: an evaluation at Vestari- Hagafellsjökull, Langjökull, Iceland: International Journal of Climatology, v. 33, no. 2, p. 410–421, doi: 10.1002/joc.3440.

Howat, I.M., Tulaczyk, S., Rhodes, P., Israel, K., and Snyder, M., 2006, A precipitation-dominated, mid-latitude glacier system: Mount Shasta, California: Climate Dynamics, v. 28, no. 1, p. 85–98, doi: 10.1007/s00382-006-0178-9.

Humlum, O., 1985, Genesis of an imbricate push moraine, Höfdabrekkujökull, Iceland: The Journal of Geology, v. 93, p. 185–195.

Johnson, M.D., and Gillam, M.L., 1995, Composition and construction of late Pleistocene end moraines, Durango, Colorado: GSA Bulletin, v. 107, no. 10, p. 1241–1253.

Johnson, P.G, 1972, A possible advanced hypsithermal position of the Donjek Glacier: Arctic, v. 25, n. 4, p. 302-305.

Karlén, W., 1973, Holocene glacier and climatic variations, Kebnekaise mountains ,Swedish Lapland: Geografiska Annaler., Series A, v. 55, no. A, p. 29–63.

Kayastha, R.B., Ageta, Y., Nakawo, M., Fujita, K., Sakai, A., and Matsuda, Y., 2003, Positive degree-day factors for ice ablation on four glaciers in the Nepalese Himalayas and Qinghai-Tibetan Plateau: Bulletin of glaciological research, v. 20,p. 7-14.

Kirkbride, M.P., 1995, Relationships between temperature and ablation on the Tasman Glacier, Mount Cook National Park , New Zealand Relationships between temperature and ablation

on the Tasman Glacier , Mount Cook National Park , N: New Zealand Journal of Geology and Geophysics, v. 38, p. 17–27.
Konya, K., Matsumoto, T., and Naruse, R., 2004, Surface heat balance and spatially distributed ablation modelling at Koryto Glacier, Kamchatka peninsula, Russia: Geografiska Annaler: Series A, v. 86, no. 4, p. 337–348.
Krüger, J., 1993, Moraine-ridge formation along a stationary ice front in Iceland: Boreas, v. 22, no. 2, p. 101–109.
Krüger, J., 1995, Origin, chronology and climatological significance of annual-moraine ridges at Myrdalsjökull, Iceland: The Holocene, v. 5, no. 4, p. 420–427.
Krüger, J., Kjær, K.H., Van Der Meer, J.J.M., 2012, From push moraine to single-crested dump moraine during a sustained glacier advance From push moraine to single-crested dump moraine during a sustained glacier advance: Norwegian Journal of Geography, no. 4, p. 37–41.
Laabs, B.J.C., Marchetti, D.W., Munroe, J.S., Refsnider, K.A., Gosse, J.C., Lips, E.W., Becker, R.A., Mickelson, D.M., and Singer, B.S., 2011, Chronology of latest Pleistocene mountain glaciation in the western Wasatch Mountains, Utah, U.S.A.: Quaternary Research, v. 76, no. 2, p. 272–284, doi: 10.1016/j.yqres.2011.06.016.
Laabs, B.J.C., Plummer, M.A., and Mickelson, D.M., 2006, Climate during the last glacial maximum in the Wasatch and southern Uinta Mountains inferred from glacier modeling: Geomorphology, v. 75, no. 3-4, p. 300–317, doi: 10.1016/j.geomorph.2005.07.026.
Laumann, T., and Reeh, N., 1993, Sensitivity to climate change of the mass balance of glaciers in southern Norway: Journal of Glaciology, v. 39, no. 133.
Li, J., Liu, S., Zhang, Y., and Shangguan, D., 2011, Surface energy balance of Keqicar Glacier, Tianshan Mountains , China , during ablation period: Sciences in Cold and Arid Regions, v. 3, no. 3, p. 197–205, doi: 10.3724/SP.J.1226.2011.00197.
Licciardi, J.M., Clark, P.U., Brook, E.J., Elmore, D., and Sharma, P., 2004, Variable responses of western U.S. glaciers during the last deglaciation: Geology, v. 32, no. 1, p. 81, doi: 10.1130/G19868.1.
Lliboutry, L., Arnao, B.M., and Schneider, B., 1977, Glaciological problems set by the control of dangerous lakes in Cordillera Blanca, Peru. III Study of moraines and mass balances at Safuna: Journal of Glaciology, v. 18, no. 79, p. 275–290.
Lyså, A. and Lønne, I., 2001, Moraine development at a small high-arctic valley glacier: Rieperbreen, Svalbard: Journal of Quaternary Science, v. 16, no. 6, p. 519–529, doi: 10.1002/jqs.613.
MacDougall, A.H., and Flowers, G.E., 2011, Spatial and temporal transferability of a distributed energy-balance glacier melt model: Journal of Climate, v. 24, p. 1480–1498, doi: 10.1175/2010JCLI3821.1.
Mair, D., Burgess, D.O., and Sharp, M.J., 2005, Thirty-seven year mass balance of Devon Ice Cap, Nunavut, Canada, determined by shallow ice coring and melt modeling: Journal of Geophysical Research, v. 110, no. F1, p. F01011, doi: 10.1029/2003JF000099.
Marshall, S.J., and Sharp, M.J., 2009, Temperature and Melt Modeling on the Prince of Wales Ice Field, Canadian High Arctic: Journal of Climate, v. 22, no. 6, p. 1454–1468, doi: 10.1175/2008JCLI2560.1.
Marshall, S., Sharp, M., Burgess, D.O., and Anslow, F.S., 2007, Near-surface-temperature lapse rates on the Prince of Wales Icefield, Ellesmere Island, Canada: Implications for

regional downscaling of temperature: International journal of …, v. 398, no. September 2006, p. 385–398, doi: 10.1002/joc.
Mihalcea, C., Mayer, C., Diolaiuti, G., Lambrecht, A., Smiraglia, C., and Tartari, G., 2006, Ice ablation and meteorological conditions on the debris-covered area of Baltoro glacier , Karakoram , Pakistan: Annals of Glaciology, v. 43, no. 1894, p. 292–300.
Oerlemans, J., Kuhn, M., Obleitner, F., Palsson, F., Smeets, C.J.P.P., Vugts, H.F., and Wolde, J.D.E., 1999, Glacio-meteorological investigations on Vatnajökull, Iceland, summer 1996: an overview: Boundary Layer Meteorology, v. 92, p. 3–26.
Oerlemans, J., and Vugts, H., 1993, A meteorological experiment in the melting zone of the Greenland ice sheet: Bulletin of the American Meteorological Society, v. 74, no. 3, p. 355–365, doi: 10.1175/1520-0477(1993)074<0355:AMEITM>2.0.CO;2.
Pellicciotti, F., Brock, B., Strasser, U., Burlando, P., Funk, M., and Corripio, J., 2005, An enhanced temperature-index glacier melt model including the shortwave radiation balance : development and testing for Haut Glacier d'Arolla, Switzerland: Journal of Glaciology, v. 51, no. 175, p. 573–587, doi: 10.3189/172756505781829124.
Petersen, L., and Pellicciotti, F., 2011, Spatial and temporal variability of air temperature on a melting glacier: Atmospheric controls, extrapolation methods and their effect on melt modeling, Juncal Norte Glacier, Chile: Journal of Geophysical Research, v. 116, no. D23, p. D23109, doi: 10.1029/2011JD015842.
Phillips, F., and Zreda, M., 1997, Cosmogenic ^{36}Cl and ^{10}Be ages of Quaternary glacial and fluvial deposits of the Wind River Range, Wyoming: GSA Bulletin, v. 109, no. 11, p. 1453–1463.
Porter, S.C., and Swanson, T.W., 2008, ^{36}Cl dating of the classic Pleistocene glacial record in the northeastern Cascade Range, Washington: American Journal of Science, v. 308, no. 2, p. 130–166, doi: 10.2475/02.2008.02.
Rabassa, J., Rubulis, S., & Suárez, J., 1979, Rate of formation and sedimentology of (1976–1978) push-moraines, Frías Glacier, Mount Tronador (41 10′ S; 71 53′ W), Argentina: Moraines and Varves, 65-79.
Roe, G.H., 2011, What do glaciers tell us about climate variability and climate change?: Journal of Glaciology, v. 57, no. 203, p. 567–578, doi: 10.3189/002214311796905640.
Roe, G.H., and O'Neal, M.A., 2009, The response of glaciers to intrinsic climate variability: observations and models of late-Holocene variations in the Pacific Northwest: Journal of Glaciology, v. 55, no. 193, p. 839–854, doi: 10.3189/002214309790152438.
Schildgen T.F., and Dethier D.P., 2000, Fire and ice: using isotopic dating techniques to interpret the geomorphic history of Middle Boulder Creek, Colorado. Geological Society of America Abstracts with Programs 32(7): 18.
Schneider, C., Kilian, R., and Glaser, M., 2007, Energy balance in the ablation zone during the summer season at the Gran Campo Nevado Ice Cap in the Southern Andes: Global and Planetary Change, v. 59, no. 1-4, p. 175–188, doi: 10.1016/j.gloplacha.2006.11.033.
Sharp, M., 1984, annual moraine ridges at Skalafellsjökull southeast Iceland: Journal of Glaciology, v. 30, no. 104, p. 82–93.
Six, D., Wagnon, P., Sicart, J.E., and Vincent, C., 2009, Meteorological controls on snow and ice ablation for two contrasting months on Glacier de Saint-Sorlin, France: Annals of Glaciology, v. 50, p. 66–72.

Steffen, K., and Box, J., 2001, Surface climatology of the Greenland ice sheet: Greenland Climate Network 1995–1999: Journal of Geophysical Research, v. 106, no. D24, p. 33951–33964.
Strasser, U., Corripio, J., Pellicciotti, F., Burlando, P., Brock, B., and Funk, M., 2004, Spatial and temporal variability of meteorological variables at Haut Glacier d'Arolla (Switzerland) during the ablation season 2001: Measurements and simulations: Journal of Geophysical Research, v. 109, p. D03103, doi: 10.1029/2003JD003973.
Szafraniec, J., 2002, Influence of positive degree − days and sunshine duration on the surface ablation of Hansbreen, Spitsbergen glacier: Polish Polar Research, v. 23, no. 3, p. 227–240.
Thorarinsson, S., 1956, On the variations of Svinafellsjökull, Skaftafellsjökull and Kviarjökull in Oraefi: Jökull, v. 6, p. 1–15.
Van den Broeke, M.R., Smeets, C.J.P.P., and Van de Wal, R.S.W., 2011, The seasonal cycle and interannual variability of surface energy balance and melt in the ablation zone of the west Greenland ice sheet: The Cryosphere, v. 5, no. 2, p. 377–390, doi: 10.5194/tc-5-377-2011.
Van de Wal, R., 1992. Ice and climate. PhD Thesis, Utrecht University, 144 pp
Ward, D.J., Anderson, R.S., Guido, Z.S., and Briner, J.P., 2009, Numerical modeling of cosmogenic deglaciation records, Front Range and San Juan mountains, Colorado: Journal of Geophysical Research, v. 114, no. F1, p. F01026, doi: 10.1029/2008JF001057.
Yong, Z., Shiyin, L., and Yongjian, D., 2007, Glacier meltwater and runoff modelling, Keqicar Baqi glacier, southwestern Tien Shan, China: Journal of Glaciology, v. 53, no. 180, p. 91–98, doi: 10.3189/172756507781833956.
Young, N.E., Briner, J.P., Leonard, E.M., Licciardi, J.M., and Lee, K., 2011, Assessing climatic and nonclimatic forcing of Pinedale glaciation and deglaciation in the western United States: Geology, v. 39, no. 2, p. 171–174, doi: 10.1130/G31527.1.
Zhang, Y., Liu, S., and Ding, Y., 2006, Observed degree-day factors and their spatial variation on glaciers in western China: Annals of Glaciology, v. 43, no. 1, p. 301–306.